Energetic Particles and the Structure of Coronal Mass Ejections

Donald V. Reames

Laboratory for High Energy Astrophysics, NASA, Goddard Space Flight Center, Greenbelt, Maryland

The largest and most energetic solar-energetic-particle (SEP) events are associated with shock waves driven out from the Sun by coronal mass ejections (CMEs). The particles from these "gradual" events are clearly distinguished from flare-associated particles by their abundances, ionization states, associations, and distributions in space and time. Multi-spacecraft observations help us map the spatial distribution of the accelerated particles that flow out into the heliosphere from the evolving CME shock or those that remain trapped behind it.

1. INTRODUCTION

Evidence of high-energy particles from the Sun was first reported 50 years ago by *Forbush* [1946], long before the first observation of coronal mass ejections (CMEs) that we now know to be the dominant source of these particles. This unfortunate quirk of history led to many years of imaginative attempts to associate the large solar energetic particle (SEP) events with solar flares, the so-called "solar flare myth" [*Gosling*, 1993]. It is only in the last ~10 years that growing new evidence from the particles themselves has allowed us to distinguish those particles from impulsive and gradual events and to associate the most intense and energetic events with CMEs, *not* with flares [*Reames*, 1990a, 1993, 1995b; *Gosling* 1993].

This paper is a review of the recent evidence on the origin of the SEP events and of the complex spatial and temporal distribution of high energy particles that accompany an evolving CME.

2. IMPULSIVE AND GRADUAL EVENTS

Nearly all of the events seen by the early observers are what we now call "proton" events or large "gradual" events, a classification originally based on the duration of the associated soft X-ray event. The time profile of such an event is shown in Figure 1a. The source region for events like this can occur at any longitude on the visible disk, as shown in Figure 2, and even far behind the west limb. Notice that it is not easy to explain such SEP observation in terms of flares, since the particles are seen for much longer than flare photons and they have great difficulty crossing magnetic field lines to distant longitudes This was "explained" by the *ad hoc* assumption of slow diffusion of particles around the corona and out into interplanetary space. It was known that SEPs often peak near interplanetary shock waves, even out near Earth, but these obviously shock-associated particles were considered to be a minor secondary process by most early workers.

In 1970 *Hsieh and Simpson* [1970] first reported ^{3}He-rich events. Such events were later found to have ^{3}He/^{4}He ratios in the range of 0.1 to 10, while the corresponding ratio in the corona and solar wind is 5×10^{-4}. Order of magnitude enhancements in heavy element abundances (e.g. Fe/O) were also seen [see *Reames, Meyer* and *von Rosenvinge*, 1994 and references therein], as compared with abundances in the solar corona or in large gradual events [see *e.g., Meyer* 1985; *Reames* 1995a]. In the 1980s we observed many of these events and found that they had time profiles like those in Figure 1b and were distributed in longitude as shown in Figure 2b. Near-relativistic electrons arrive only slightly after the photons in these impulsive events, and give good associations with

Coronal Mass Ejections
Geophysical Monograph 99

Published in 1997 by the American Geophysical Union

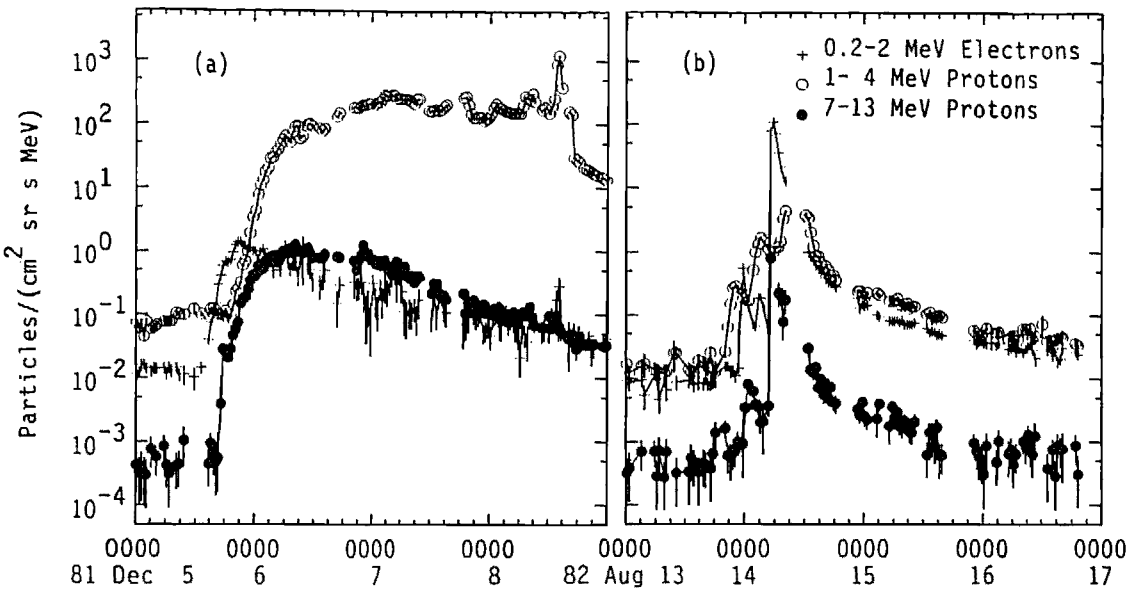

Figure 1. Time profiles of protons and electrons in *(a)* gradual (proton) event and in *(b)* impulsive (^{3}He-rich) events.

impulsive flares and type III radio bursts [*Reames et al.* 1988; *Reames, Cane,* and *von Rosenvinge,* 1990].

Thus, the particles that clearly came from impulsive flares showed only modest spread in longitude and time, contradicting the tremendous diffusion postulated for the large gradual events. The long time duration of the gradual events *must* be coming from continuing acceleration at an interplanetary shock; the longitude distribution screams "shock" to all who would listen. Shocks can easily cross field lines that particles cannot and they can accelerate the particles as they go. Since *Kahler et al.* [1984] showed a 96% correlation between proton events and CMEs, acceleration must occur at the CME-driven shock; blast-wave shocks, that are un-correlated with CMEs, must play little role.

The large gradual event shown in Figure 1a is one I show often since it comes from a well-known disappearing-filament event [*Kahler et al.* 1986] which has a CME but no associated flare. Such events show that no flare is required to produce a large particle event at 1 AU, nor is one required to provide "seed particles" for subsequent shock acceleration. Much of our progress in understanding the physical processes that occur in impulsive and gradual events has come from studying these smaller "pure" events with CMEs but no flares or with impulsive flares but no CMEs. The largest events are very complex and are plagued by "big flare syndrome" [*Kahler* 1982] so it is difficult to determine conclusively which particles are related to which phenomena at the Sun.

Even more compelling evidence for the origin of the particles in gradual events is found in the measurements of the ionization states of the elements C through Fe that are now measured by four different experiment groups on three different spacecraft over energies ranging from 0.3 to 600 MeV/amu. Table 1 summarizes the ionization states for Fe, the element most sensitive to the source plasma temperature. These ionization states are typical of plasma temperatures in the range 1 - 2 MK, like the ambient corona and solar wind. Even the C and O are not fully ionized in gradual events. Similar ionization states are measured for the ions of the solar wind itself. It is clear that the energetic ions do not come from hot plasma near a flare or reconnection region where temperatures exceed 10 MK and Fe XXV spectral lines are often seen. Even at the highest energies, the ions in gradual events are accelerated from the ambient corona and solar wind, far from a flare.

In contrast, a mean ionization state of Fe of 20 5±1.2 was found for impulsive-flare (^{3}He-rich) events [*Luhn et al.* 1987], indicating an electron temperature of >10 MK.

Not only do the energetic ions in gradual events originate at ambient coronal temperatures, but those above about ~10 MeV/amu would be further ionized by passing through dense coronal material. At the highest energies the Fe ions would be measurably stripped of additional

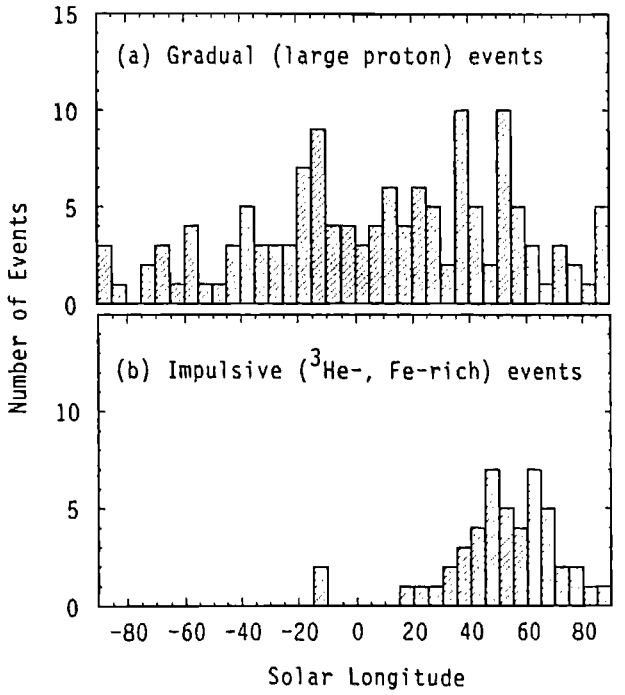

Figure 2. Longitude distribution of *(a)* gradual and *(b)* impulsive events [*Reames* 1995b].

electrons in less than 1 sec at a density of 10^{10} atoms cm^{-3} found in the low corona. The ionization time is much shorter than the acceleration time at this density. According to *Lee* and *Ryan* [1986] a time of tens of minutes is required to accelerate ions to GeV energies; this requires that the acceleration take place at a density of 10^7 atoms cm^{-3} or less to avoid stripping the energetic Fe.

Other evidence that high-energy particles are accelerated relatively far from the Sun has been presented by *Kahler* [1994]. He plots the solar injection intensity of particles as a function of the height of the leading edge of the CME, as shown in Figure 3. For most of the energies shown, the particle intensities approach a broad maximum beyond 12 $R_\odot$, while even at 21 GeV they peak between 5-10 $R_\odot$. In the 1989 September 29 event shown, the leading edge of the CME is observed to move at >1800 km/s.

Table 2 summarizes the properties of impulsive and gradual events. The two particle populations are clearly distinguished in their combined properties: events with the abundance signature of impulsive events have impulsive time profiles (like Figure 1b), come from well-connected flares, have type III radio bursts, impulsive X-ray profiles, rarely have associated CMEs, *etc.* However, both particle

Table 1. Mean Ionization States of Energetic Fe in Large Gradual Events

MeV/amu	Q_{Fe}	Events	Reference
0.3 - 2	14.1±0.2	12	Luhn et al. 1987
0.5 - 5	11.0±0.2	2	Mason et al. 1995
15 - 70	15.2±0.7	2	Leske et al. 1995
200 - 600	14.1±1.4	3	Tylka et al. 1995

populations can occasionally be seen in a large event where both physical processes occur. In these cases, an Fe-rich population is seen early in the event from the impulsive phase, followed by Fe-poor material from the gradual phase [*Reames* 1990b]. *Cliver* [1996] has described these events as having a core and a halo, composed of particles from the impulsive and gradual populations, respectively. In some cases the Fe-rich flare component can be quite intense [*Van Hollebeke, McDonald and Meyer* 1990].

3. IMPULSIVE-FLARE EVENTS

It is presently thought that the characteristic abundance enhancements in impulsive events are produced by resonant wave-particle interactions in the flare plasma Streaming 10-100 keV electrons, that are seen *via* the type III radio bursts and hard X-rays they produce, form velocity distributions that are unstable for production of hydrogen electromagnetic ion cyclotron (EMIC) waves [*Temerin and Roth* 1992]. These wave frequencies lie between the gyrofrequencies of H and of ^{4}He. The rare isotope ^{3}He is the only species whose gyrofrequency lies in this range to resonantly absorb these waves. EMIC waves are only produced in regions of high magnetic field near the base of the corona where the Alfvén speed is >2000 km/s (and in the Earth's aurorae where electrons, waves and ions are all measured). The acceleration is so efficient that the observed number of ^{3}He ions in space requires the acceleration of >10% of the ^{3}He in a typical flare volume near the base of the corona [*Reames* 1993]. The more modest enhancements of heavy elements are produced when these ions resonate with harmonics of these waves or with other wave modes [*Miller and Viñas* 1993].

In a few cases it has been possible to deduce ion abundances of the beam trapped on closed coronal loops from the broad γ-ray line intensities observed. These abundances show the same pattern of enhancements of ^{3}He, Ne, Mg, Si and Fe as are seen in the impulsive-flare particles we observe at 1 AU [*Murphy et al.* 1991].

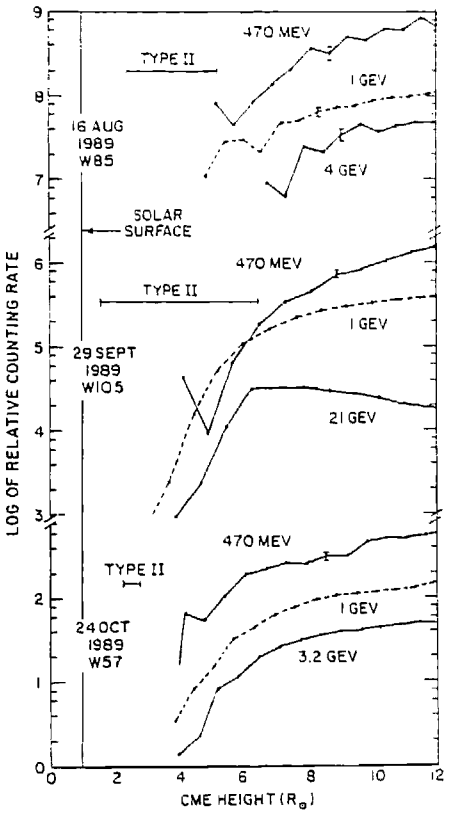

Figure 3. Source injection intensity of GeV particles *vs.* height of the leading edge of the CME [*Kahler* 1994].

Table 2. Properties of Impulsive and Gradual Events

	Impulsive	Gradual
Particles:	Electron-rich	Proton-rich
$^3He/^4He$	~ 1	~ 0.0005
Fe/O	~ 1	~ 0.1
H/He	~ 10	~ 100
Q_{fe}	~ 20	~ 14
Duration	Hours	Days
Longitude Cone	<30 deg	~180 deg
Radio Type	III, V (II)	II, IV
X-rays	Impulsive	Gradual
Coronagraph	-	CME (96%)
Solar Wind	-	IP Shock
Events/year	~1000	~10

4. PROTON EVENTS AND CME-DRIVEN SHOCKS

4.1 Shock Acceleration Profiles

To set a framework for understanding the time profiles of the shock-accelerated particles, it is useful to review briefly the theory of diffusive shock acceleration [see *Lee* 1983]. As accelerated particles stream away from a shock they generate Alfvén waves that resonantly scatter subsequent particles of that energy so as to reduce the streaming. These particles then scatter back and forth across the shock, gaining energy on each transit. As they stream outward at a higher energy they generate waves resonant at this new energy, *etc.* At a given energy an equilibrium is established so that the intensity of particles and resonant waves depends only on distance from the shock. This intensity pattern decreases with distance from the shock. Such patterns are observed near shock passage and are called "energetic storm particle (ESP)" events for historical reasons. Direct observations of both particles and waves have confirmed the predictions of the *Lee* [1983] theory at low energies where the measurements are easily made

At some distance from the shock, particle intensities become too low to generate enough waves and they stream freely outward. This can lead to the flat profile shown in Figure 4a that is often seen in MeV particles. To understand this flat profile, suppose a shock wave accelerates some fraction of the local solar wind plasma to the energy of interest and the particles then expand like R^{-2} as they come out to the observer. If the source solar wind density also varies like R^{-2}, the intensity seen by an observer at distance R from the Sun will not vary with time. The intensity value of the flat profile is determined by saturation of the wave-particle equilibrium and is empirically found to be several x 100 protons $(cm^2\ sr\ s\ MeV)^{-1}$ in the few MeV region [*Reames* 1990b]. This value was found consistent with theory by *Ng* and *Reames* [1994]. Their Table 2 shows that order-of-magnitude increases in particle intensity near the sun have little effect on intensities at 1 AU after this saturation value is reached.

At higher energies there may be too few particles to generate waves as the shock expands, so acceleration efficiency may decrease with time, leading to a profile more like the one shown in Figure 4b. At sufficiently high energy (or for a sufficiently weak shock) the ESP bump may not survive out to 1 AU, although cases of ESP events in ~500 MeV protons at 1 AU are known.

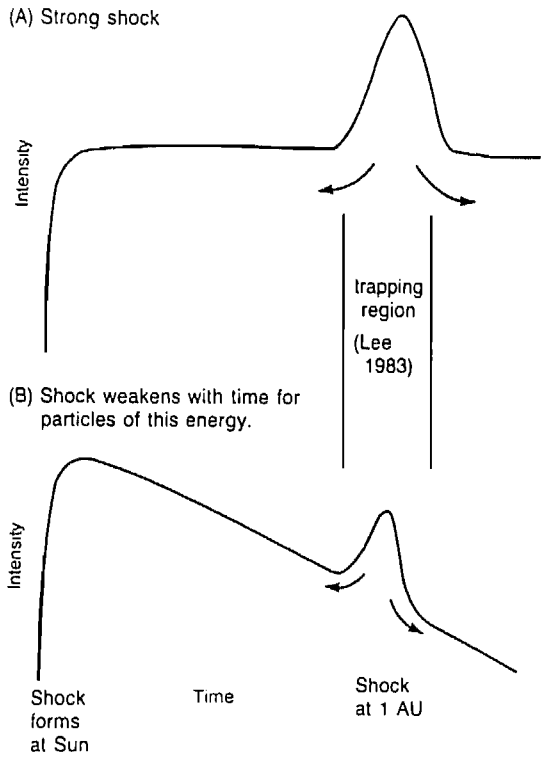

Figure 4. Intensity-time profiles for particles from shock acceleration that *(a)* remains constant out to the observer and *(b)* diminishes with time [*Reames, Barbier,* and *Ng* 1996].

4.2 Longitude Distributions

The foregoing discussion assumes that the observer remains magnetically connected to the same point on a shock as it propagates out to 1 AU. Unfortunately, this is never the case and the particle profiles are strongly affected because the observer's magnetic connection point sweeps across the face of the shock. This means that an observer viewing a CME from central meridian will nominally be connected 55° to the west of the source when it is near the Sun and the shock will first encounter his field line at right angles. As the CME moves outward, his connection point will swing across the face of the shock until he is connected to the nose of the shock when it arrives at 1 AU.

An observer viewing a CME at W55° will be directly connected to the nose of the shock when it leaves the Sun, but will be 55° around on its eastern flank when it arrives at 1 AU. Finally, the observer of an eastern event will see an improving connection with time, but he will only become connected to the nose of the shock after he crosses the local shock and arrives on field lines that connect to the nose of the shock from behind.

The pattern of typical particle intensity-time profiles resulting from these geometric effects is shown in Figure 5 The observer viewing a CME nearly head-on (E01°) sees flat time profiles after a slow rise, especially from a wide CME. The observer on the eastern flank sees a W53° event which peaks early, when he is connected to the nose of the shock, and long before shock arrival. For the observer on the western flank, viewing an E45° event, the particle intensities rise slowly as the magnetic connection improves, but peak intensity does not occur until the observer is behind the local shock on field lines that connect him to its nose.

4.3 Multi-Spacecraft Observations

The original study of particle profiles as a function of longitude leading to Figure 5 was done by *Cane, Reames,* and *von Rosenvinge* [1988] by examining profiles of 235 proton events (obtained over 20 years) in different source-longitude intervals. However, the sizes of CMEs and the strength of shocks differ greatly, so it is important to study the spatial distribution of particles around a single CME shock. A recent study, using spatially separated spacecraft, has been performed by *Reames, Barbier,* and *Ng* [1996].

Particle profiles in a fairly small gradual event are shown in Figure 6. The inset in the figure shows the spatial distribution of the *Helios 1, Helios 2,* and *IMP 8* spacecraft relative to the CME which is projecting downward, just as it was shown in the cartoon in Figure 5 In the upper panel of Figure 6, the profile seen at the centrally-located *Helios 1* shows a gradual rise to a plateau, followed by a pronounced ESP peak precisely at the time of shock passage. *Helios 2* and *IMP 8* are connected increasingly far around on the west flank of the shock. Their intensities slowly increase as their connection point swings eastward with time, but their intensities do not reach maximum until well after shock passage. This shock must have a steep gradient in intensity with longitude around from the nose.

The 30-45 MeV protons in the lower panel of Figure 6 have a similar pattern of rise until the shock reaches ~0 4 AU (for *Helios 1*) then the intensity begins to fall. This is understood as weakening in the acceleration efficiency with time as discussed in connection with Figure 4b.

Notice that long after shock passage the intensities at all spacecraft reach the same value that then decreases with time. This behavior is seen at all energies in all of the events where it could be studied. Behind the CME is a large, spatially uniform population of particles that is trapped in an expanding magnetic bottle [see *Reames, Barbier,* and *Ng* 1996].

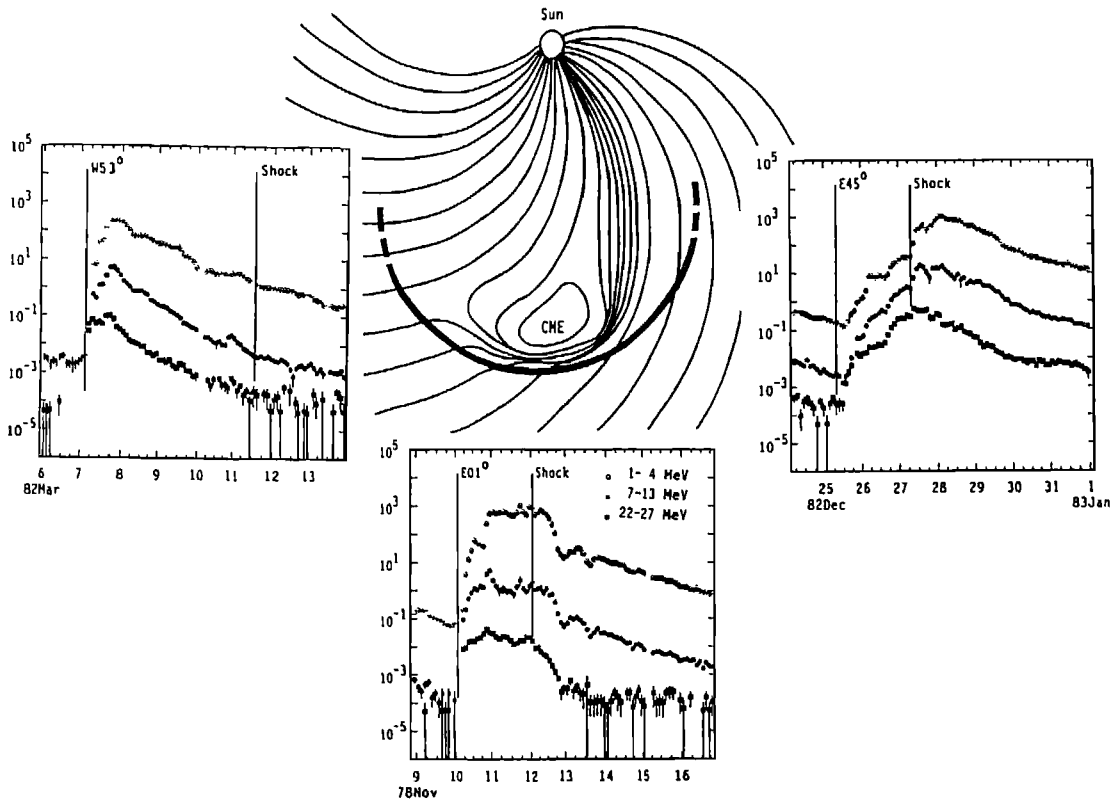

Figure 5. Intensity profiles for protons of different energy for observers viewing a CME from the three different longitudes indicated in the panels [*Reames, Barbier,* and *Ng* 1996].

A much larger event is shown in Figure 7. Despite a much wider separation of the spacecraft (*Helios 2* is 108° west of the source and its connection longitude is ~160° to the west), the intensities rise much more rapidly at all of the spacecraft and they remain high until after shock passage at all energies. This event has a broad shock front with little intensity variation along it. The shock continues to accelerate protons at least to 45 MeV out to 1 AU and beyond Again, the intensities at all three spacecraft approach the same value late in the event when the shock and CME are beyond about 2 AU.

We can follow this same event further in time and space in Figure 8 where we see a second increase in intensity when the west flank of the shock re-encounters the field lines somewhere near *Voyager* causing a new increase there and sending a new burst of particles inward toward *IMP 8* [see *Reames, Barbier,* and *Ng* 1996] The intensities at the two spacecraft differ greatly during the first peak owing to an ~R^{-3} expansion of the peak intensity of particle distribution [*e.g. Parker* 1963]; the peak is delayed and broadened by particle scattering over the ~10 AU path length along the field. Intensities are similar on the second peak. The dip in the intensities at both spacecraft near October 1 tells us that the shock does not cover 360° with equal intensity; this decrease occurs after the east flank of the shock leaves the field line and before the west flank re-encounters it.

These enormous shocks propagate outward through the heliosphere, crossing and re-crossing each field line. Often, the strongest shocks overtake and merge with previous weaker ones, continuing to accelerate particles to the boundaries of the heliosphere.

Behind each large shock is a quasi-trapped population of particles that is spatially uniform in both longitude and radius over a large fraction of the inner heliosphere. As the bottle containing these particles expands, their intensity decreases adiabatically but their abundances and energy spectral shapes remain largely unaffected [*Reames, Barbier* and *Ng* 1996; *Reames et al.* 1996]. To some extent these particles also form a reservoir or seed-population that is available for re-acceleration and can continually feed the shock from behind.

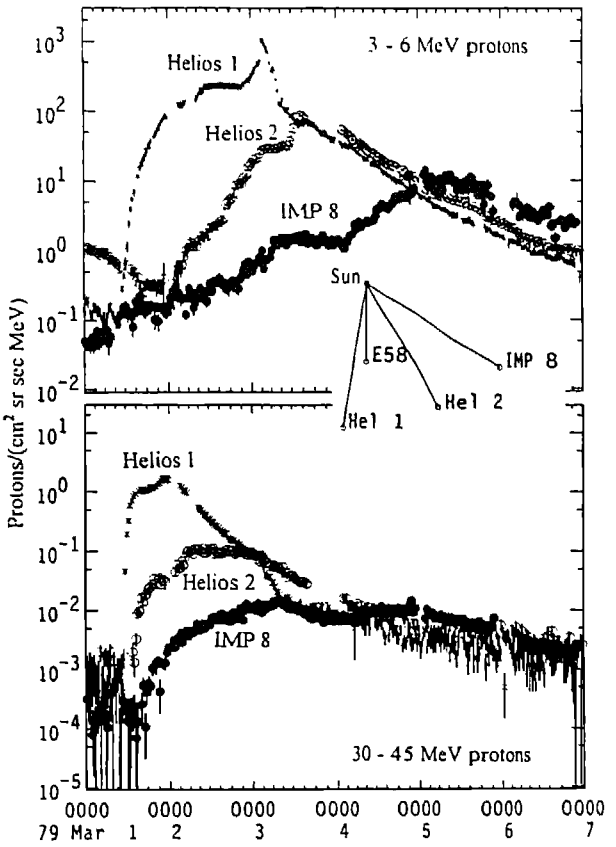

Figure 6. The spatial distribution of particles around a small gradual event as observed by three spacecraft [*Reames, Barbier,* and *Ng* 1996].

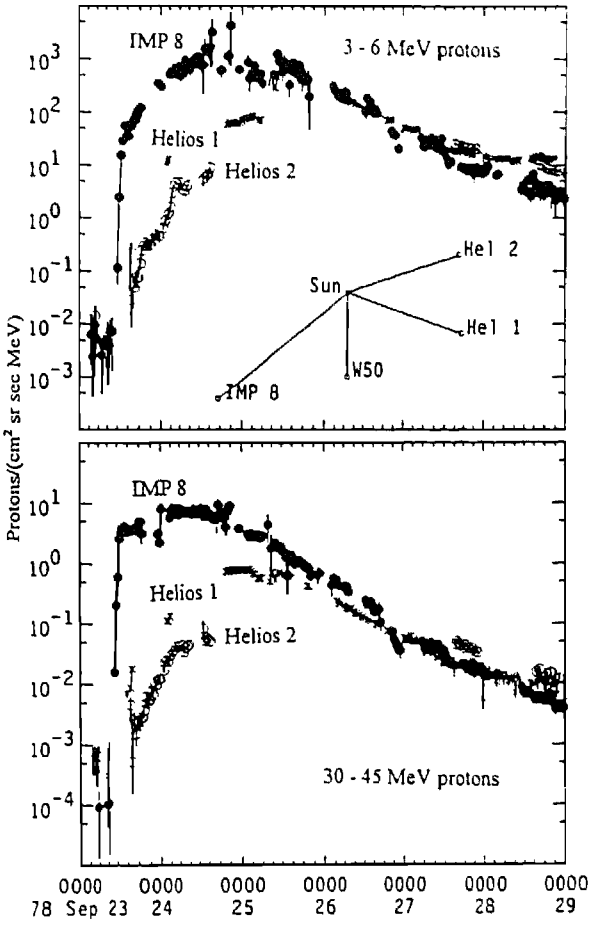

Figure 7. Intensities at widely separated spacecraft in the large event of 1978 September 23 show much less variation with longitude [*Reames, Barbier,* and *Ng* 1996].

4 4 Probing the Magnetic Cloud

Inside magnetic clouds in large events one finds a plateau in the proton intensity at a few percent of the intensity just ahead of the cloud (see 1978 Nov 13 in Figure 5). It is possible that the particles gain access to this closed field region by reconnection of a few percent of the internal field lines with external lines that thread the shock. This is also the region where bi-directional flows of ions and electrons are seen [*e. g. Richardson and Reames* 1993] as will be discussed elsewhere in this book.

However, new injections of particles from impulsive flares back at the Sun serve to probe the magnetic topology of this region [*Kahler and Reames* 1991]. The very existence of these particles tells us that at least one end of the field line is connected to the Sun, *i.e.* that *this* cloud is not a detached plasmoid. Very sensitive new measurements on the WIND spacecraft of the magnetic cloud of 1995 October 19 show a large number of tiny impulsive events that fill the cloud with Fe-rich material [*Reames et al* 1996]. The electron observations in this cloud show a spatial patchwork of magnetic filaments that are alternately connected to and disconnect from the Sun [*Larson et al* 1996].

When we examine the temporal distribution of impulsive events we find that they often occur in clusters from flares in a single active region; these clusters are frequently found in and behind a CME. We think this correlation is a consequence of the global geometry of the interplanetary magnetic field. Most of the field in interplanetary space has diverged out of coronal holes. However, flares do not occur in coronal holes, they occur in active regions. One of the best places to find field lines that connect to active regions where flares occur is in a magnetic cloud that has been ejected from an active region as part of a CME.

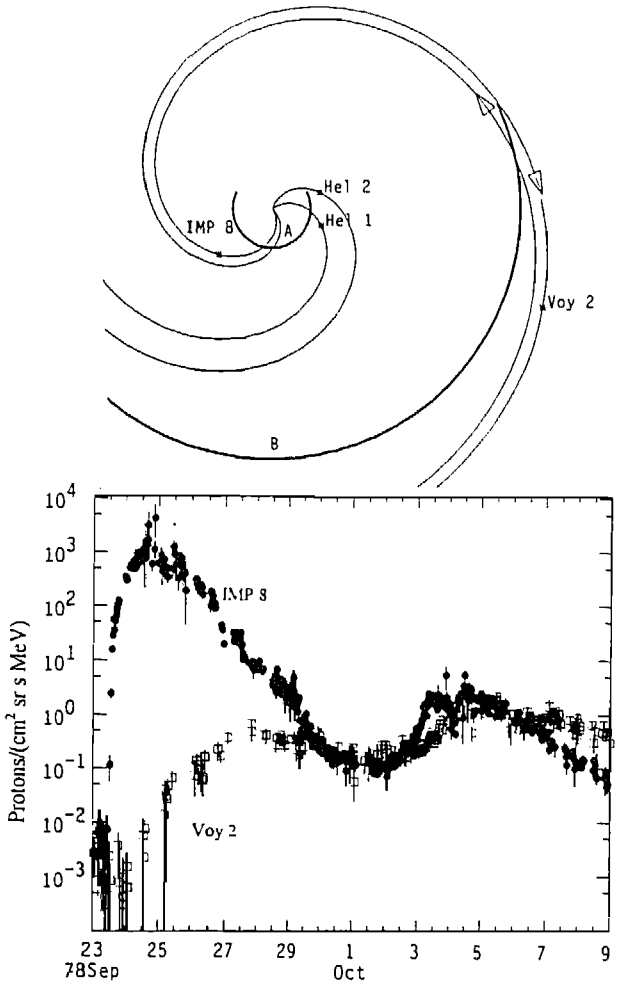

Figure 8. An expanded view of the 1979 September 23 event shows a second increase when the western flank of the shock re-encounters the field line connecting *IMP 8* and *Voyager 2* near 4 AU [adapted from *Reames, Barbier,* and *Ng* 1996].

It is important to note that the CME driver gas is *not* the source of the shock-accelerated ions. According to *Boberg, Tylka and Adams* [1996], the source gas for the accelerated ions is the *coronal* material overlying the CME rather than interplanetary material swept up at a later time. In the later phases, of course, an important source of high-energy particles may be those lower-energy particles accelerated earlier that have been trapped in and behind the shock.

5. CONCLUSIONS

Two distinct mechanisms are responsible for acceleration of the particles we observe in SEP events: 1) stochastic acceleration by resonant wave-particle interactions in the low corona in impulsive flares and 2) diffusive shock acceleration of the ambient plasma of the high corona and solar wind by the shock wave driven outward by a CME The particle populations from each source can be distinguished, even when both mechanisms occur in a single large event.

The largest events, containing most of the particles seen at 1 AU, are gradual events that come from the CME shock source. Many particles are also accelerated in flares but most are trapped on flare loops and those that escape do so in a limited longitude region near the flare.

In large events many of the observed phenomena are, or appear to be, correlated. For example, X-rays are produced in the corona behind a CME, probably by electrons accelerated during magnetic reconnection. Meanwhile, protons and ions are accelerated at the shock in front of the CME. Thus protons are associated with long-duration X-ray events, which is the reason we call these events gradual. However, the fact that proton events are correlated with certain X-ray properties such as duration and, more recently, with a pattern of X-ray spectral hardening, does *not* imply that protons are accelerated at the same time and place as the electrons that produce X-rays. It only means that different phenomena occur in different parts of big fast CMEs.

Particle acceleration is strongest near the nose of the CME-driven shock. In most events it can decrease rapidly away from the nose, depending on the speed and longitude span of the CME. (In extremely large, powerful events the longitude gradients are more modest.) An observer's point of connection scans across the face of this shock with time leading to large intensity variations that are caused solely by this geometric effect. Western (eastern) events always have intensity maxima prior to (after) shock passage, because that is when the spacecraft is magnetically connected to the nose of the shock. Relatively few events, only those with the CME launched near central meridian, show the intensity peak exactly at the nose of the shock.

The energetic protons and other ions accelerated in gradual events are virtually invisible in photons. X-rays and radio emission are produced by electrons, not ions, and the acceleration occurs in low-density plasma where interactions are much too rare to produce either measurable X-rays or γ-rays. It is ironic that the most intense and pervasive particle events in the inner heliosphere can only be studied by direct *in situ* measurements of the particles themselves.

The flare myth dies hard. Most of us learned as students that SEP events came from flares and we learned our les-

sons well. Flares are familiar and easy to see. An army of physicists have dedicated careers to an intensive study of flares for over 100 years. However, the particles themselves have told a new and compelling story about the plasma from which they come. Most of them clearly do *not* come from flares, but from CME shocks; objections to this picture have withered as more measurements have been made. Once we accepted this origin we began to look for and find the rich spatial structure in the evolving SEP events that rivals that of the CMEs themselves. Even though we cannot image an SEP event, we can begin to appreciate the structure that such an image might reveal.

I would like to thank Chee K. Ng for numerous helpful discussions and Tycho von Rosenvinge for his comments on this manuscript.

REFERENCES

Boberg, P. R., A. J. Tylka, and J. H. Adams, Solar energetic Fe charge state measurements: Implications for acceleration by coronal mass ejection-driven shock, *Astrophys. J. (Letters)*, 471, L65, 1996.

Cane, H. V., D. V. Reames, and T. T. von Rosenvinge, The role of interplanetary shocks in the longitude distribution of solar energetic particles, *J. Geophys. Res.*, 93, 9555, 1988.

Cliver, E. W., Solar flare gamma-ray emission and energetic particles in space, in *High Energy Solar Physics*, edited by R. Ramaty, N, Mandzhavidze and X.-M. Hua, pp 45-60, AIP Conf. Proc 374, AIP press, Woodbury, NY, 1996

Forbush, S. E., Three unusual cosmic-ray increases possibly due to charged particles from the Sun, *Phys. Rev.*, 70, 771, 1946.

Gosling, J. T., The solar flare myth, *J. Geophys. Res.*, 98, 18949, 1993.

Hsieh, K. C., and J. A. Simpson, The relative abundances and energy spectra of ^{3}He and ^{4}He from solar flares, *Astrophys. J. (Letters)*, 162, L191, 1970.

Kahler, S. W., The role of the big flare syndrome in correlations of solar energetic proton fluxes and associated microwave burst parameters, *J. Geophys. Res.* 87, 3439, 1982.

Kahler, S. W., Injection profiles for solar energetic particles as functions of coronal mass ejection heights, *Astrophys. J.* 428, 837, 1994.

Kahler, S. W., E. W. Cliver, H. V. Cane, R. E. McGuire, R. G. Stone and N. R. Sheeley, Solar filament eruptions and energetic particle events, *Astrophys. J.* 302, 504, 1986.

Kahler, S. W., and D. V. Reames, Probing the magnetic topologies of magnetic clouds by means of solar energetic particles, *J. Geophys. Res.*, 96, 9419, 1991.

Kahler, S. W., N. R. Sheeley, Jr., R. A. Howard, M. J. Koomen, D. J. Michels, R. E. McGuire, T. T. von Rosenvinge, and D. V. Reames, Associations between coronal mass ejections and solar energetic proton events, *J. Geophys. Res.* 89, 9683, 1984.

Larson, D. E., R. E. Ergun, J. M. McTiernan, R. P. Lin, J. P McFadden, C. W. Carlson, K. A. Anderson, M. McCarthy, G Parks, H. Reme, J. M. Bosqued, K.-P. Wenzel, and T. R Sanderson, Wind spacecraft observations of energetic particles in the October 1995 magnetic cloud, to be published, 1996

Lee, M. A., Coupled hydromagnetic wave excitation and ion acceleration at interplanetary traveling shocks, *J. Geophys Res.*, 88, 6109, 1983

Lee, M. A. and J. M. Ryan, Time-dependent coronal shock acceleration of energetic solar flare particles, *Astrophys. J 303*, 829, 1986.

Leske, R. A., J. R. Cummings, R. A. Mewaldt, E. C. Stone, and T. T. von Rosenvinge, Measurements of the ionic charge states of solar energetic particles using the geomagnetic field, *Astrophys J. (Letters) 452*, L149, 1995.

Luhn, A., B. Klecker, D. Hovestadt, and E. Mobius, The mean ionic charge of silicon in ^{3}He-rich solar flares, *Astrophys J*, 317, 951, 1987.

Mason, G. M., J. E. Mazur, M. D. Looper, and R. A. Mewaldt, Charge state measurements of solar energetic particles with SAMPEX, *Astrophys. J. 452*, 901 (1995)

Meyer, J. P., The baseline composition of solar energetic particles, *Astrophys. J.* Suppl., 57, 151, 1985.

Miller, J. A. and A. F. Viñas, Ion acceleration and abundance enhancements by electron beam instabilities in impulsive solar flares, *Astrophys. J.*, 412, 386, 1993.

Murphy, R. J., R. Ramaty, B. Kozlovsky, and D. V. Reames, Solar abundances from gamma-ray spectroscopy: comparisons with energetic particles and photospheric abundances *Astrophys. J.*, 371, 793, 1991.

Ng, C. K. and Reames, D. V., Focused interplanetary transport of ~1 MeV solar energetic protons through self-generated Alfvén waves, *Astrophys. J.* 424, 1032, 1994.

Parker, E. N., *Interplanetary Dynamical Processes*, (Interscience Publ., New York) 1963.

Reames, D. V., Energetic particles from impulsive solar flares, *Astrohys. J. Suppl.*, 73, 235, 1990a.

Reames, D. V., Acceleration of energetic particles by shock waves from large solar flares, *Astrophys. J. (Letters)*, 358, L63, 1990b.

Reames, D. V., Non-thermal particles in the interplanetary medium, Adv. Space Res., 13 (No. 9), 331, 1993.

Reames, D. V., Coronal abundances determined from energetic particles, *Adv. Space Res. 15*, No.7, 41, 1995a.

Reames, D. V., Solar energetic particles: a paradigm shift, *Revs Geophys Suppl. 33*, 585, 1995b.

Reames, D. V., L. M. Barbier, and C. K. Ng, The spatial distribution of particles accelerated by coronal mass ejection-driven shocks, *Astrophys. J. 466*, 473, 1996.

Reames, D. V., L. M. Barbier, T. T. von Rosenvinge, G. M Mason, J. E. Mazur, and J. R. Dwyer, Energy spectra of ions accelerated in impulsive and gradual solar flares, *Astrophys J*, submitted 1996.

Reames, D. V., H. V. Cane, and T. T. von Rosenvinge, Energetic particle abundances in solar electron events, *Astrophys J*, 357, 259, 1990.

Reames, D. V., B. R. Dennis, R. G. Stone, and R. P. Lin, X-ray and radio properties of solar ^{3}He-rich events, *Astrophys. J.* 327, 998, 1988.

Reames, D. V., J. P. Meyer, and T. T. von Rosenvinge, Energetic-particle abundances in impulsive solar-flare events, *Astrophys. J. Suppl.*, 90, 649, 1994.

Richardson, I. G., and D. V. Reames, Bidirectional ~1 MeV/amu ion intervals in 1973-1991 observed by the Goddard Space Flight Center instruments on IMP-8 and ISEE-3/ICE, *Astrophys J. Suppl.* 85, 411, 1993.

Temerin, M. and I. Roth, The production of ^{3}He and heavy ion enrichments in ^{3}He-rich flares by electromagnetic hydrogen ion cyclotron waves, *Astrophys. J. (Letters)* 391, L105, 1992.

Tylka, A. J., P. R. Boberg, J. H. Adams, Jr., L. P. Beahm, W F Dietrich, and T. Kleis, The mean ionic charge state of solar energetic Fe ions above 200 MeV/nucleon, *Astrophys J (Letters) 444*, L109 (1995).

Van Hollebeke, M. A. I.., F. B. McDonald, and J. P. Meyer, Solar energetic particle observations of the 1982 June 3 and 1980 June 21 gamma-ray/neutron events, *Astrophys. J. Suppl.*, 73, 285, 1990.

D. V. Reames, Code 661, NASA, Goddard Space Flight Center, Greenbelt, MD 20771 (email: reames@lheavx.gsfc.nasa.gov)